Coupled channels in the distorted-wave representation

I. Bray and I. E. McCarthy
Institute for Atomic Studies, The Flinders University of South Australia, Bedford Park, South Australia 5042, Australia

J. Mitroy
Department of Theoretical Physics, Australian National University, Canberra, Australian Capital Territory 2600, Australia

K. Ratnavelu
Institute for Atomic Studies, The Flinders University of South Australia, Bedford Park, South Australia 5042, Australia
(Received 27 December 1988)

The scattering of electrons or positrons to discrete states of an atomic target is represented in momentum space by coupled integral equations. By introducing a local central potential one may set up a distorted-wave representation for the integral equations, which can be solved to arbitrary numerical accuracy by quadratures. The perturbative solutions of these equations are the commonly used distorted-wave first- and second-order Born approximations. The full coupled on-shell solution is the distorted-wave unitarized Born approximation. These approximations are tested for charged and uncharged targets. The formalism for inclusion of configuration interaction in the target is described, making a complete theory for electron-atom scattering in a truncated channel space, which can be extended by optical potentials to a fully realistic situation.

I. INTRODUCTION

The momentum-space solution of the coupled equations of electron-atom scattering theory has some useful features. Given a numerical method of solving a set of coupled integral equations one needs only to calculate the driving and kernel elements, which are all Born approximation amplitudes, usually off shell. The set of coupled equations is truncated to include only discrete target states. The continuum is included in the form of an *ab initio* optical potential, which involves low-order approximations to the continuum wave functions.

The momentum-space coupled-channels optical method for electron scattering from hydrogenic targets was discussed in detail by McCarthy and Stelbovics[1] (hereafter referred to as I). Here the potential matrix elements were expressed in the plane-wave representation, so that the driving terms of the integral equations were plane-wave Born amplitudes. The use of the distorted-wave representation for elastic scattering was discussed by Mitroy, McCarthy, and Stelbovics.[2]

In the present work the distorted-wave representation is applied to coupled channels, the formalism for multielectron atoms is given explicitly, and the case of charged targets is treated in the Coulomb-wave representation. A short-range distorting potential is not used for charged targets because of numerical difficulties.

One useful feature of the momentum-space treatment is that it enables the assessment of some of the common approximations of scattering theory[3] by applying them to the distorted-wave solution of the integral equations in a truncated channel space, considered as a model scattering problem. The driving terms of the integral equations in the distorted-wave representation are the amplitudes of the distorted-wave Born approximation (DWBA). The first iteration of the integral equations produces the distorted-wave second-order Born approximation (DWSB). Both these approximations are in common use for electron-atom scattering. Their use here differs slightly from that for a realistic scattering problem. First, the intermediate states in DWSB are here restricted to the model space, whereas for a realistic problem approximations are made for the entire space of target states. Second, the integral equations cannot be closed with distorting potentials chosen differently for different channels, as is often done. The distorting potential here is only a means of accelerating numerical convergence and it is chosen with computational simplicity in mind.

Another simplification is the distorted-wave unitarized Born approximation (UDWB), in which the real parts of the Green's functions in the integral equations are set equal to zero, so that the solution involves a set of algebraic linear equations with on-shell DWBA amplitudes. These approximations can all be compared to the complete solution of the integral equations for the truncated channel space. Their advantage is a saving of computer time.

The method of solving the set of coupled integral equations used here is the same as that discussed in I. An important feature of the distorted-wave representation for elastic scattering[2] was that the number of quadrature points necessary to solve the equations accurately was much less than for the plane-wave representation, so that there was much less reason in terms of computing time to

make low-order approximations. This is investigated here for coupled channels.

Section II discusses the coupled integral equations. In Sec. III we discuss the computation of cross sections in the distorted-wave representation. In Sec. IV we give the formalism for the potential matrix elements in the case of many-electron targets. Configuration interaction is included in terms of the m-scheme density-matrix elements obtained from a structure calculation.[4] In Sec. V we use the example of scattering from the $3s$ and $3p$ states of sodium in the Hartree-Fock approximation to compare the plane-wave and distorted-wave representations for solving the coupled-channels problem at 54.42 and 200 eV. In Sec. VI the sodium example at 54.42 eV is used to compare different approximations to the coupled-channels solution. Section VII discusses scattering from the $1s$, $2s$, and $2p$ states of He^+ as an example of the momentum-space solution for a charged target.

II. COUPLED INTEGRAL EQUATIONS

The coupled integral equations for a total energy E are written for a truncated set of channels projected by the operator P. The target states concerned are denoted by p and p'

$$(\varepsilon_p - H_T)|p\rangle = 0 , \tag{1}$$

where H_T is the target Hamiltonian. We include the complementary channel space, projected by the operator Q, by adding a complex nonlocal term to the first-order electron-target potential V, giving the optical potential $V^{(Q)}$.

The transition and potential matrices are represented in terms of the eigenstates of the real, local, central potential U. These eigenstates include continuum distorted waves $|\mathbf{k}^{(\pm)}\rangle$, with outgoing and ingoing spherical-wave boundary conditions, respectively, and bound states $|\lambda\rangle$, defined by

$$(E^{(\pm)} - \varepsilon_p - K - U)|\mathbf{k}^{(\pm)}\rangle = 0 , \tag{2}$$

$$(\varepsilon_\lambda - K - U)|\lambda\rangle = 0 , \tag{3}$$

where K is the kinetic energy operator.

U is chosen to describe as much of the electron-target scattering as possible. In this work

$$U = \langle p|V|p\rangle , \tag{4}$$

i.e., the average of the first-order electron-target potential V for the initial target state p. For the case of a charged target, U must include the Coulomb potential due to the residual charge Z. In this work for charged targets U is chosen to be exactly the Coulomb potential

$$U(r) = -Z/r . \tag{5}$$

The coupled integral equations for the distorted-wave T-matrix elements are written, suppressing the conserved total orbital angular momentum and spin quantum numbers J and S,

$$\begin{aligned}
\langle \mathbf{k}'^{(-)} p'|T|p\mathbf{k}^{(+)}\rangle &= \langle \mathbf{k}'^{(-)} p'|V^{(Q)} - U|p\mathbf{k}^{(+)}\rangle + \sum_{p''\in P} \int d^3q \langle \mathbf{k}'^{(-)} p'|V^{(Q)} - U|p''\mathbf{q}^{(-)}\rangle \\
&\quad \times \frac{1}{E^{(+)} - \varepsilon_p'' - \frac{1}{2}q^2} \langle \mathbf{q}^{(-)} p''|T|p\mathbf{k}^{(+)}\rangle \\
&\quad + \sum_{p''\in P} \sum_{\lambda'} \langle \mathbf{k}'^{(-)} p'|V^{(Q)} - U|p''\lambda'\rangle \frac{1}{E^{(+)} - \varepsilon_p'' - \varepsilon_\lambda'} \langle \lambda' p''|T|p\mathbf{k}^{(+)}\rangle , \\
\langle \lambda p'|T|p\mathbf{k}^{(+)}\rangle &= \langle \lambda p'|V^{(Q)} - U|p\mathbf{k}^{(+)}\rangle + \sum_{p''\in P} \int d^3q \langle \lambda p'|V^{(Q)} - U|p''\mathbf{q}^{(-)}\rangle \frac{1}{E^{(+)} - \varepsilon_p'' - \frac{1}{2}q^2} \langle \mathbf{q}^{(-)} p''|T|p\mathbf{k}^{(+)}\rangle \\
&\quad + \sum_{p''\in P} \sum_{\lambda'} \langle \lambda p'|V^{(Q)} - U|p''\lambda'\rangle \frac{1}{E^{(+)} - \varepsilon_p'' - \varepsilon_\lambda'} \langle \lambda' p''|T|p\mathbf{k}^{(+)}\rangle .
\end{aligned} \tag{6}$$

The equations (6) are solved in angular-momentum-projected form. We give the angular-momentum projection of the T matrix, which applies similarly to V. All quantum numbers are displayed explicitly:

$$\begin{aligned}
&\langle \mathbf{k}'^{(-)} p'|T^{(JS)}|p\mathbf{k}^{(+)}\rangle \\
&= \sum_{L',M',N',L,M,N,J,K,S,N_S} \langle \hat{\mathbf{k}}'|L'M'\rangle (L'M'l'm'|JK)(\tfrac{1}{2}N's'n'|SN_S) T_{l'l}^{(JS)}(k',k) (LMlm|JK)(\tfrac{1}{2}Nsn|SN_S) \langle LM|\hat{\mathbf{k}}\rangle .
\end{aligned} \tag{7}$$

The notation used for the quantum numbers and momenta is set out fully in Table I. Unprimed and primed quantities represent the initial and final states, respectively. The symbols in parentheses are Clebsch-Gordan coefficients and

$$\langle \hat{\mathbf{k}}|LM\rangle = Y_{LM}(\hat{\mathbf{k}}) . \tag{8}$$

The index I in (7) is the L-channel index. It represents the partial-wave orbital angular momentum L of the continuum electron and the set of target quantum numbers p.

TABLE I. Notation for quantities used in the formalism. Initial and final states are denoted, respectively, by unprimed and primed quantities. The third column in the matrix element table gives the angular-momentum (AM) projection of the matrix element. DW stands for distorted wave.

Quantity	State vectors (angular-momentum projection) Definition	Label	Orbital	Spin
channel state	$\|kpJKSN_S\rangle$	kp	JK	SN_S
target state	$\|plmsn\rangle$	p	lm	sn
projectile partial wave	$\|kLMN\rangle$	k	LM	$\frac{1}{2}N$
L channel	$\|Lp\rangle$	I		
single-particle state	$\|il_im_in_i\rangle$	i	l_im_i	$\frac{1}{2}n_i$
orbital	$\|\alpha l_\alpha\rangle$	α	$l_\alpha(m_\alpha)$	$\frac{1}{2}(n_\alpha)$

Type	Matrix elements Three-dimensional notation	AM projection
driving: continuum DW	$\langle \mathbf{k}'^{(-)}p'\|V^{(Q)}-U\|p\mathbf{k}^{(+)}\rangle$	$\bar{V}^{(JS)}_{I'I}(k',k)$
driving: bound state of U	$\langle \lambda p'\|V^{(Q)}-U\|p\mathbf{k}^{(+)}\rangle$	$\bar{V}^{(JS)}_{I'I}(\lambda,k)$
kernel: continuum DW	$\langle \mathbf{k}'^{(-)}p'\|V^{(Q)}-U\|p''\mathbf{q}^{(-)}\rangle$	$\bar{V}^{(JS)}_{I'I''}(k',q)$
kernel: bound state of U	$\langle \lambda p'\|V^{(Q)}-U\|p''\mathbf{q}^{(-)}\rangle$	$\bar{V}^{(JS)}_{I'I''}(\lambda,q)$
total T matrix	$\langle \mathbf{k}'p'\|\tilde{T}\|p\mathbf{k}\rangle$	$\tilde{T}^{(JS)}_{I'I}(k',k)$
DW T matrix: continuum	$\langle \mathbf{k}'^{(-)}p'\|T\|p\mathbf{k}^{(+)}\rangle$	$T^{(JS)}_{I'I}(k',k)$
DW T matrix: bound state	$\langle \lambda p'\|T\|p\mathbf{k}^{(+)}\rangle$	$T^{(JS)}_{I'I}(\lambda,k)$
Scattering amplitude for U	$\langle \mathbf{k}'p\|U\|p\mathbf{k}\rangle$	$t^{(JS)}_I(k)\delta_{I'I}$

For each channel p, I takes values corresponding to partial waves L that satisfy the conservation of orbital angular momentum

$$|J-l|\le L\le J+l \tag{9}$$

and the conservation of parity. In the case of a target that is not an orbital-angular-momentum singlet, Eqs. (6) have either natural parity

$$\Pi(J)=\Pi(L+l) \tag{10}$$

or unnatural parity

$$\Pi(J+1)=\Pi(L+l)\ . \tag{11}$$

The use of the T-matrix element in calculating cross sections is described in Sec. III.

III. CROSS SECTIONS IN THE DISTORTED-WAVE REPRESENTATION

The differential cross section for electron scattering from initial target state p to final target state p' in a state of total spin S is

$$\frac{d\sigma^{(S)}_{p'p}}{d\Omega}=(2\pi)^4\frac{k'}{k}\frac{2S+1}{2(2s+1)(2l+1)}\sum_{m',m}|\langle \mathbf{k}'p'|\tilde{T}|p\mathbf{k}\rangle|^2\ . \tag{12}$$

The notation for the quantum numbers and other quantities used in this section is described in Table I. The initial and final electron momenta are $\mathbf{k}$ and $\mathbf{k}'$, respectively (atomic units are used throughout) and $\tilde{T}$ is the T matrix for the problem. For simplicity the spin index S is suppressed in the notation for $\tilde{T}$. It is useful for comparison with calculations[5] that we use the S matrix to note that

$$S=1-2\pi i(k'k)^{1/2}\tilde{T}\ . \tag{13}$$

The matrix element of $\tilde{T}$ is expressed in terms of the distorted-wave T-matrix element $\langle \mathbf{k}'^{(-)}p'|T|p\mathbf{k}^{(+)}\rangle$ of Eq. (6) by a transformation due to Gell-Mann and Goldberger,[6]

$$\langle \mathbf{k}'p'|\tilde{T}|p\mathbf{k}\rangle=\langle \mathbf{k}'^{(-)}p'|T|p\mathbf{k}^{(+)}\rangle+\langle \mathbf{k}'|t|\mathbf{k}\rangle\delta_{p'p}\ , \tag{14}$$

where t is the T matrix for elastic scattering by the distorting potential U. The partial-wave matrix elements of $\tilde{T}$ are expressed in the abbreviated notation of Eq. (7),

$$\tilde{T}^{(JS)}_{I'I}(k',k)=T^{(JS)}_{I'I}(k',k)+t^{(JS)}_I(k)\delta_{I'I}\ . \tag{15}$$

In practice we choose $\hat{\mathbf{k}}$ to be the angular quantization axis and calculate the $\tilde{T}$-matrix element in the form

$$\langle \mathbf{k}'p'|\tilde{T}|p\mathbf{k}\rangle = \sum_{J=0}^{J_0}\sum_{L,L'}(4\pi)^{-1/2}\hat{L}(L'M'l'm'|Jm)\times(L0lm|Jm)\tilde{T}^{(JS)}_{I'I}(k',k)Y_{L'M'}(\hat{k}')\ , \tag{16}$$

where

$$\hat{L}=(2L+1)^{1/2}\ . \tag{17}$$

If the distorting potential U is zero (plane-wave representation) we may sum the J series to infinity by using the fact that

$$\tilde{T}^{(JS)}_{I'I}(k',k)=V^{(JS)}_{I'I}(k',k),\quad J>J_0,\quad I'\neq I\ . \tag{18}$$

We normally take $J_0=80$. For such J_0 values the exchange matrix elements of the first-order potential V are negligible. We add and subtract the first-order V-matrix element and calculate the $\tilde{T}$-matrix element in the form

$$\langle \mathbf{k}'p'|\tilde{T}|p\mathbf{k}\rangle=\langle \mathbf{k}'p'|\tilde{T}-V|p\mathbf{k}\rangle+\langle \mathbf{k}'p'|V|p\mathbf{k}\rangle \ , \qquad (19)$$

where the partial-wave matrix elements of the first term are zero for $J>J_0$. This method of including all the higher partial waves is very accurate except for elastic scattering, where coupling to dipole channels results in long-range polarization potentials. This is handled by an analytic approximation[7] to the elastic T-matrix element. The subtraction technique (19) is not used for scattering from charged targets. The only analytic forms for the Coulomb-Born matrix element are very complicated and have not been implemented. Other experimental quantities, such as total and total reaction cross sections and angular-correlation parameters, are calculated conventionally using $\tilde{T}$.

IV. POTENTIAL MATRIX ELEMENTS

The target atom is described by the nucleus, a closed-shell inert core of electrons, and a number of active (valence) electrons. Quantum numbers associated with the target description are described fully by Table I. A target state p is described in terms of orbitals α by a configuration-interaction expansion obtained by diagonalizing the Hamiltonian in a truncated set of configurations. Each configuration is a determinant of single-particle states i, the unexcited configuration being the Hartree-Fock determinant. The projection-independent part of the single-particle state i is the orbital α. For the excited configurations used, only the active electrons may be in single-particle states unoccupied in the Hartree-Fock configuration.

The potential matrix elements for all electrons include the potential for one positive charge from the nucleus. This eliminates the Rutherford singularity. The residual asymptotic charge in the case of an ion target is included in the distorting potential U.

The partial-wave expansions of the distorted-wave potential matrix elements require three types of coordinate representation of distorted waves, which differ only by phase factors in the case of real potentials. For optical potentials we treat the real and imaginary parts separately:

$$\begin{aligned}
\langle \mathbf{r}|\mathbf{k}^{(+)}\rangle&=(2/\pi)^{1/2}(kr)^{-1}\\
&\quad\times\sum_{L,M} i^L e^{i(\sigma_L+\delta_L)}u_L(k,r)\langle \hat{\mathbf{r}}|LM\rangle\langle LM|\hat{\mathbf{k}}\rangle \ ,\\
\langle \mathbf{r}|\mathbf{k}^{(-)}\rangle&=(2/\pi)^{1/2}(kr)^{-1}\\
&\quad\times\sum_{L,M} i^L e^{-i(\sigma_L+\delta_L)}u_L(k,r)\langle \hat{\mathbf{r}}|LM\rangle\langle LM|\hat{\mathbf{k}}\rangle \ ,\\
\langle \mathbf{k}^{(-)}|\mathbf{r}\rangle&=(2/\pi)^{1/2}(kr)^{-1}\\
&\quad\times\sum_{L,M} i^{-L} e^{i(\sigma_L+\delta_L)}u_L(k,r)\langle \hat{\mathbf{k}}|LM\rangle\langle LM|\hat{\mathbf{r}}\rangle \ ,
\end{aligned} \qquad (20)$$

where σ_L is the Coulomb phase shift, $u_L(k,r)$ is real, and the external form of the partial wave is

$$e^{i\delta_L}u_L(k,r)=F_L(kr)+(2i)^{-1}(e^{2i\delta_L}-1)\times[G_L(kr)+iF_L(kr)] \ , \qquad (21)$$

with F_L and G_L being the regular and irregular Coulomb functions. For brevity the phase shifts will be omitted from the following expressions for matrix elements.

The angular-momentum-projected solution of the integral equations (6) requires potential matrix elements defined for channels p and partial-wave angular momenta L. The target states p are defined as linear combinations of products of single-particle states i. We can calculate radial potential matrix elements for orbitals α. They must be related to the channel matrix elements by orbital-channel coefficients. These coefficients are simplest for the direct matrix elements. We will consider them first.

We express the potential matrix element in second-quantized form, using annihilation operators $a_{\mathbf{k}}$ and the corresponding creation operators for electrons with momentum $\mathbf{k}$. The annihilation operator for a bound electron in a single-particle state i is a_i. Operating on the ground state $|0\rangle$ the creation operator $a_{\mathbf{k}}^\dagger$ produces a distorted wave with appropriate boundary conditions, which is denoted henceforth for brevity by $|\mathbf{k}\rangle$,

$$a_{\mathbf{k}}^\dagger|0\rangle=|\mathbf{k}\rangle \ . \qquad (22)$$

The channel matrix element is

$$\begin{aligned}
\langle \mathbf{k}'p'|V|p\mathbf{k}\rangle&=\langle 0p'|a_{\mathbf{k}'}Va_{\mathbf{k}}|p0\rangle\\
&=\langle 0p'|a_{\mathbf{k}'}\sum_{i,j,\mathbf{q}',\mathbf{q}} a_i^\dagger a_{\mathbf{q}'}^\dagger a_{\mathbf{q}}a_j a_{\mathbf{k}}^\dagger\\
&\quad\times\langle \mathbf{q}'i|V|j\mathbf{q}\rangle|p0\rangle \ .
\end{aligned} \qquad (23)$$

The summation sign represents a momentum integration where appropriate.

A. Direct potential

Using the fermion commutation rules the direct-channel matrix element reduces to

$$\langle \mathbf{k}'p'|V_D|p\mathbf{k}\rangle=\sum_{i,j}\langle p'|a_i^\dagger a_j|p\rangle\times[\langle \mathbf{k}'|\mathcal{V}-U|\mathbf{k}\rangle\delta_{ij}+\langle \mathbf{k}'i|v|j\mathbf{k}\rangle] \ , \qquad (24)$$

where the configuration-interaction structure is represented by the m-scheme density-matrix elements $\langle p'|a_i^\dagger a_j|p\rangle$ and the single-particle excitation matrix element has been split into two terms. The first contains the central potential $\mathcal{V}-U$, where $\mathcal{V}$ includes the core direct potential and the residual Coulomb potential $-Z/r$, and U is the distorting potential. The second is the interaction with valence electrons.

The simplification for the direct potential occurs because the direct excitation operator is spin independent and spin-projection quantum numbers occur only in the form

$$\langle n_i | n_j \rangle = \delta_{n_\alpha n_\beta} . \tag{25}$$

Since we are using the orbital notation α for the projection-independent part of the single-particle state i we prefer to use α and β rather than i and j to denote the single-particle quantum numbers.

The orbital angular-momentum part of the direct excitation operator is a tensor operator T^λ_μ, where λ is the multipole index of the Coulomb potential v, and μ is its projection.

It is convenient to eliminate all projection quantum numbers from the formalism, restoring them when the three-dimensional $\bar{T}$-matrix elements are computed by (16). This is done by using the Wigner-Eckart theorem for tensor operators in orbital and spin space (LS coupling):

$$\langle l'm's'n' | T^{\lambda\sigma}_{\mu\nu} | lmsn \rangle = (-1)^{l'-m'} \begin{pmatrix} l' & \lambda & l \\ -m' & \mu & m \end{pmatrix} (-1)^{s'-n'} \times \begin{pmatrix} s' & \sigma & s \\ -n' & \nu & n \end{pmatrix} \langle l's' \| \mathbf{T}^{\lambda\sigma} \| ls \rangle . \tag{26}$$

Here the symbols in parentheses are the Wigner $3j$ symbols. $T^{\lambda\sigma}_{\mu\nu}$ is a tensor with space and spin polarities λ and σ and space and spin projections μ and ν, respectively. For orbital angular momentum the reduced matrix elements are

$$\langle l_\alpha \| \mathbf{C}^\lambda \| l_\beta \rangle = (-1)^{l_\alpha} \hat{l}_\alpha \hat{l}_\beta \begin{pmatrix} l_\alpha & \lambda & l_\beta \\ 0 & 0 & 0 \end{pmatrix} , \tag{27}$$

where we use the renormalized spherical harmonics

$$C^\lambda_\mu(\hat{\mathbf{k}}) = [4\pi/(2\lambda+1)]^{1/2} \langle \hat{\mathbf{k}} | \lambda\mu \rangle . \tag{28}$$

The target-state matrix element is

$$\langle p' | T^\lambda_\mu | p \rangle = \sum_{i,j} \langle p' | a_i^\dagger a_j | p \rangle \langle i | T^\lambda_\mu | j \rangle . \tag{29}$$

The m-scheme density matrix is written, expanding the notation for the single-particle state i to display the projection quantum numbers explicitly,

$$\langle p' | a_i^\dagger a_j | p \rangle = \rho_{\alpha m_\alpha n_\alpha, \beta m_\beta n_\beta}(p',p) . \tag{30}$$

We apply the Wigner-Eckart theorem, defining the reduced density matrix $\rho^\lambda_{\alpha\beta}(p',p)$ by

$$\sum_{m_\alpha, n_\alpha, m_\beta, n_\beta} (-1)^{l_\alpha - m_\alpha} \begin{pmatrix} l_\alpha & \lambda & l_\beta \\ -m_\alpha & \mu & m_\beta \end{pmatrix} \times \rho_{\alpha m_\alpha n_\alpha, \beta m_\beta n_\beta}(p',p) = (-1)^{l'-m'} \begin{pmatrix} l' & \lambda & l \\ -m' & \mu & m \end{pmatrix} \rho^\lambda_{\alpha\beta}(p',p) . \tag{31}$$

The direct-potential matrix element is

$$V^{(JS)}_{I'I}(k',k) = \sum_\lambda (-1)^{L+l'+J} \begin{Bmatrix} L & l & J \\ l' & L' & \lambda \end{Bmatrix} \langle L' \| \mathbf{C}^\lambda \| L \rangle \times \sum_{\alpha,\beta} [R^\lambda_{\alpha\beta}(k',k) + \delta_{\lambda 0} W(k',k)] \times \langle l_\alpha \| \mathbf{C}^\lambda \| l_\beta \rangle \rho^\lambda_{\alpha\beta}(p',p) , \tag{32}$$

where the symbol in braces is a Wigner $6j$ symbol. The radial matrix element $W(k',k)$ comes from all the direct central potential contributions. They are the core potential $V_{\text{core}}(r)$ and the residual Coulomb potential $-Z/r$. The distorting potential $U(r)$ is subtracted.

$$W(k',k) = \frac{2i^{L-L'}}{\pi k' k} \int_0^\infty dr\, u_{L'}(k',r) u_L(k,r) \times [V_{\text{core}}(r) - Z/r - U(r)] \tag{33}$$

and the valence radial matrix element is

$$R^\lambda_{\alpha\beta}(k',k) = \frac{2i^{L-L'}}{\pi k' k} \int_0^\infty dr_1 u_{L'}(k',r_1) u_L(k,r_1) \times \int_0^\infty dr_2 u_\alpha(r_2) u_\beta(r_2) \frac{r^\lambda_<}{r^{\lambda+1}_>} . \tag{34}$$

For small $\lambda \neq 0$ the radial matrix element (34) involves long-range integrals proportional to $r^{-\lambda-1}$ whose integrands are not zero in the tail region beyond the point r_0 at which the bound-state orbitals u_α and u_β are negligible. We write it in the form

$$R^\lambda_{\alpha\beta}(k',k) = \frac{2i^{L-L'}}{\pi k' k} \left[\int_0^{r_0} dr_1 V^\lambda_{\alpha\beta}(r_1) u_{L'}(k',r_1) \times u_L(k,r_1) + \gamma^\lambda_{\alpha\beta} t^\lambda_{L'L}(r_0) \right] , \tag{35}$$

where the direct potential is

$$V^\lambda_{\alpha\beta}(r_1) = r_1^{-(\lambda+1)} \int_0^{r_1} dr_2 r_2^\lambda u_\alpha(r_2) u_\beta(r_2) + r_1^\lambda \int_{r_1}^\infty dr_2 r_2^{-(\lambda+1)} u_\alpha(r_2) u_\beta(r_2) , \tag{36}$$

the coefficient of the radial-tail integral is

$$\gamma^\lambda_{\alpha\beta} = (1-\delta_{\lambda 0}) \int_0^\infty dr_2 r_2^\lambda u_\alpha(r_2) u_\beta(r_2) , \tag{37}$$

and the radial-tail integral is

$$t^\lambda_{L'L}(r_0) = \int_{r_0}^\infty dr_1 r_1^{-(\lambda+1)} u_{L'}(k',r) u_L(k,r_1), \quad \lambda > 0 . \tag{38}$$

The radial-tail integrals are evaluated in the uncharged case using the external form of the partial waves $u_L(k,r)$. This involves spherical Bessel and Neumann functions for which the corresponding integrals can be evaluated analytically[8] over the range r_0 to infinity. For the charged case only the integration of the regular Coulomb function from zero to infinity is sufficiently simple analytically.[9–11] The integration range zero to r_0 is treated by

the same quadrature as is used for (35). The difficulty of evaluating the integral for the irregular Coulomb function precludes the use of a short-range distorting potential for charged targets.

B. Exchange potential

The exchange-channel matrix element is

$$\langle \mathbf{k}'p'|V_E|p\mathbf{k}\rangle = -\langle \mathbf{k}'p'|H-E|\mathbf{k}p\rangle = \left\langle \mathbf{k}'p' \left| E-H_T-K_0-\mathcal{V}-v-\sum_{\mu(\neq 1)} v_\mu \right| \mathbf{k}p \right\rangle , \quad (39)$$

where K_0 is the projectile kinetic energy operator, H_T is the target Hamiltonian, v is the interaction of the projectile (0) and active (1) electrons, and v_μ is the interaction of the projectile with an electron that acts as a spectator in the transition $p \rightarrow p'$.

We first consider the valence exchange term v in (39). We now have the complication of spin exchange. The reduced density-matrix appropriate to this case is a matrix representation of a tensor operator formed by coupling $a_i^\dagger$ and a_j to orbital quantum numbers j, m_j and spin quantum numbers σ, ν. The tensor operator is

$$[a_\alpha^\dagger \times a_\beta]^{j\sigma}_{m_j\nu} = \sum_{m_\alpha, n_\alpha, m_\beta, n_\beta} (-1)^{l_\beta - m_\beta} (l_\alpha m_\alpha l_\beta - m_\beta | j m_j)(-1)^{1/2-n_\beta} (\tfrac{1}{2} n_\alpha \tfrac{1}{2} - n_\beta | \sigma\nu) a^\dagger_{\alpha m_\alpha n_\alpha} a_{\beta m_\beta n_\beta} . \quad (40)$$

We now use the Wigner-Eckart theorem (26), defining the reduced density matrix $\rho^{j\sigma}_{\alpha\beta}(p',p)$ by

$$\langle p'|[a_\alpha^\dagger \times a_\beta]^{j\sigma}_{m_j\nu}|p\rangle = (-1)^{l'-m'} \begin{pmatrix} l' & j & l \\ -m' & m_j & m \end{pmatrix} (-1)^{s'-n'} \begin{pmatrix} s' & \sigma & s \\ -n' & \nu & n \end{pmatrix} \rho^{j\sigma}_{\alpha\beta}(p',p) . \quad (41)$$

The angular-momentum-projected valence-exchange matrix element is

$$V^{(JS)}_{l'l}(k',k) = \sum_{\lambda,j,\sigma} (-1)^{s'+S+(1/2)} \hat{S}^2 \hat{\sigma} \begin{Bmatrix} s' & s & \sigma \\ \frac{1}{2} & \frac{1}{2} & S \end{Bmatrix} (-1)^{l_\alpha + l' + J + j + 1} \hat{J}^2 \hat{j} \times \begin{Bmatrix} L' & L & j \\ l_\alpha & l_\beta & \lambda \end{Bmatrix} \begin{Bmatrix} L' & L & j \\ l & l' & J \end{Bmatrix} \sum_{\alpha,\beta} R^\lambda_{\alpha\beta}(k',k) \langle l_\alpha \| \mathbf{C}^\lambda \| L \rangle \langle L' \| \mathbf{C}^\lambda \| l_\beta \rangle \rho^{j\sigma}_{\alpha\beta}(p',p) . \quad (42)$$

The exchange radial matrix element is

$$R^\lambda_{\alpha\beta}(k',k) = \frac{2i^{L-L'}}{\pi k' k} \int_0^\infty dr_1 \int_0^\infty dr_2 u_{L'}(k',r_1) u_L(k,r_2) \times u_\alpha(r_2) u_\beta(r_1) \frac{r_<^\lambda}{r_>^{\lambda+1}} . \quad (43)$$

In addition to valence exchange there are one-body matrix elements due to further terms in (39). The first is valence-overlap exchange, where the electrons μ are valence electrons. In the exchange matrix element for independent-particle configurations Φ', Φ we may operate on the exchanged configuration (in which electron 0 is bound) with the Hartree operator

$$\left[K_0 + \mathcal{V} + \sum_{\mu(\neq 1)} v_\mu\right] |\Phi\rangle = \varepsilon_\Phi |\Phi\rangle . \quad (44)$$

For the term of the determinant Φ containing the electron 0 in orbital α, ε_Φ is equal to the orbital energy ε_α to a good approximation. We make this approximation in (39). In order to obtain a symmetric matrix element we add two halves with the electron 0 in Φ and Φ', respectively. The radial matrix element contribution to (43) is

$$R^\lambda_{\alpha\beta}(k',k) = -\frac{2i^{L-L'}}{\pi k' k} [E - \tfrac{1}{2}(\varepsilon_{p'} + \varepsilon_p + \varepsilon_\alpha + \varepsilon_\beta)] \times (u_\alpha | u_{L'})(u_L | u_\beta) \delta_{\lambda 0} , \quad (45)$$

where the parentheses indicate radial overlap integrals and we have used Eq. (1) for the operation of H_T.

In addition to the exchange terms (43) and (45) for the active electrons there are exchange terms due to the closed-shell core. Only half of the electrons in each shell contribute for each incident spin projection N so the multiplicity for orbital α is $2l_\alpha + 1$. The core-exchange potential is central. For the v term in (39) the core-exchange term is the one-orbital reduction of (42),

$$V^{(JS)}_{II}(k',k) = -(2l_\alpha + 1) \sum_\lambda \begin{pmatrix} L & \lambda & l_\alpha \\ 0 & 0 & 0 \end{pmatrix}^2 R^\lambda_{\alpha\alpha}(k',k) , \quad (46)$$

where the radial matrix element is given by (43). The remaining terms in (39) contribute to the core-overlap exchange. This is the diagonal form of (45). The α contribution is

$$V^{(JS)}_{II}(k',k) = \frac{2i^{L-L'}}{\pi k' k} (E - \varepsilon_p - \varepsilon_\alpha) \times (u_\alpha | u_{L'})(u_L | u_\alpha) \delta_{\lambda 0} . \quad (47)$$

For economy of notation we have used the same name for each of the different exchange contributions. Terms of the same name are added.

V. COMPARISON OF PLANE- AND DISTORTED-WAVE REPRESENTATIONS

The computational differences between plane- and distorted-wave representations are minor. They concern only the radial partial waves $u_L(k,r)$ in the direct and exchange radial matrix elements (34) and (43), (45), (46), and (47). For plane waves the $u_L(k,r)$ are Riccati-Bessel functions. For Coulomb waves they are the regular Coulomb functions $F_L(k,r)$. When the short-range distorting potential U is included they are calculated by solving the radial scattering equation for the potential U. In these three cases the radial tail integrals (38) for small multipoles can be calculated using analytic expressions for the range zero to infinity. In addition the Coulomb- and distorted-wave representations include radial matrix elements in which $u_L(k,r)$ is replaced by a bound-state wave function $u_\lambda(r)$ which is either a bound Coulomb function or an eigenfunction of the potential U.

Alternatively, the direct radial matrix element (34) can be calculated as an angular-momentum projection of the analytic Born matrix element in the plane-wave case.[1] For large values of L the oscillations of the Legendre polynomial make this a less accurate method than (34).

The example used for comparison of the plane- and distorted-wave representations is the coupled $3s$ and $3p$ channels for sodium in the Hartree-Fock approximation. The distorting potential is the static potential of the $3s$ ground state. This potential supports three bound states (two s type and one p type), which are included in the off-shell quadrature mesh. The bunching transformations for the quadrature points are chosen according to the usual criteria and are not specially optimized.

Table II is a study of the convergence with the number of quadrature points of the T-matrix elements in the distorted- and plane-wave representations for $J=0,1,2$. It also shows the unitarized Born approximation in each case (UDWB and UBA), the first-order (DWBA and FBA) and the second-order (DWSB and SBA) solutions. The second-order solutions are shown for 24-point quadratures.

At both 200 and 54.42 eV the 24-point and 16-point calculations for distorted waves agree to better than 1%. This is true also for 12 points at 200 eV and it is not much worse at 54.42 eV. At 200 eV there is not much to choose between UDWB and DWSB results, both agreeing with the coupled-channel (CC) results to better than 5% for the larger T-matrix elements. The DWBA result is not much worse than this. Departures from CC results are a little larger for 54.42 eV and the UDWB result is better than the DWSB result. In general the table shows that 12-point quadratures are quite satisfactory for the distorted-wave representation.

For the plane-wave representation the T-matrix elements seem to be converging to the limit of the distorted-wave representation as the number of quadrature points increases, but in many cases even the 24-point plane-wave T-matrix elements are not as close to the distorted-wave limit as the 12-point distorted-wave values. Neither the first- nor second-order solutions are good enough even as a rough first approximation. The same is true for the UBA.

Another interesting feature of the table is that it demonstrates the on-shell convergence of the perturbation solutions of the distorted-wave representation. In fact, the iteration of the whole solution of the coupled integral equations does not converge in any of the cases shown, but this is due to some of the off-shell matrix elements. The iterative solution usually converges for $J>3$. For these low values of J plane-wave perturbation theory is not convergent in any sense.

A feature of the table is that the unitarized distorted-wave Born approximation, which couples on-shell amplitudes exactly but ignores off-shell amplitudes completely, is a better approximation in this case than the distorted-wave second-order Born approximation, which treats both on- and off-shell amplitudes up to second order.

TABLE II. T-matrix elements (magnitude and phase) for electron scattering in the $3s,3p$ model of sodium. Upper entries in each case are for the distorted-wave representation, lower entries for the plane-wave representation.

E_0 (eV)	J	Channel	24 points	16 points	12 points	UBA	FBA	SBA
200	0	$3s$	0.0535,−2.368	0.0537,−2.364	0.0536,−2.366	0.0521,−2.399	0.0550,−2.461	0.0540,−2.376
		singlet	0.0540,−2.369	0.0543,−2.356	0.0589,−2.318	0.0473,−2.535	0.0576,π	0.0720,−2.551
		$3p$	0.0156,−0.226	0.0157,−0.223	0.0156,−0.229	0.0146,−0.245	0.0154,−0.520	0.0161,−0.242
		singlet	0.0147,−0.196	0.0156,−0.217	0.0131,−0.205	0.0015,1.185	0.0021,0	0.0036,0.905
		$3s$	0.0530,−2.385	0.0532,−2.381	0.0531,−2.383	0.0524,−2.396	0.0554,−2.457	0.0544,−2.373
		triplet	0.0542,−2.366	0.0553,−2.353	0.0655,−2.230	0.0474,−2.533	0.0578,π	0.0729,−2.557
		$3p$	0.0145,−0.234	0.0147,−0.231	0.0146,−0.240	0.0142,−0.233	0.0150,−0.520	0.0157,−0.231
		triplet	0.0146,−0.194	0.0142,−0.165	0.0030,−0.093	0.0015,1.179	0.0022,0	0.0040,0.851
	1	$3s$	0.0653,−0.974	0.0652,−0.973	0.0652,−0.972	0.0656,−0.975	0.0688,−0.936	0.0648,−0.962
		singlet	0.0649,−0.972	0.0636,−0.950	0.0678,−1.051	0.0452,−2.565	0.0540,π	0.0802,−2.687
		$3p-$	0.0093,2.917	0.0094,2.920	0.0093,2.915	0.0087,2.913	0.0091,2.625	0.0099,2.905
		singlet	0.0096,2.931	0.0098,2.961	0.0112,2.878	0.0015,1.233	0.0023,0	0.0039,0.972

TABLE II. (*Continued*).

E_0 (eV)	J	Channel	24 points	16 points	12 points	UBA	FBA	SBA
		$3p+$	0.0116,−3.060	0.0116,−3.062	0.0116,−3.070	0.0115,−3.069	0.0121,−3.350	0.0122,−3.057
		singlet	0.0123,−3.056	0.0125,−3.023	0.0127,−3.119	0.0006,1.184	0.0009,0	0.0021,2.540
		$3s$	0.0652,−0.970	0.0651,−0.968	0.0651,−0.967	0.0655,−0.970	0.0687,−0.932	0.0647,−0.957
		triplet	0.0645,−0.959	0.0635,−0.947	0.0670,−1.025	0.0455,−2.560	0.0545,π	0.0809,−2.682
		$3p-$	0.0091,2.934	0.0091,2.928	0.0090,2.922	0.0084,2.920	0.0088,2.625	0.0095,2.913
		triplet	0.0094,2.950	0.0100,2.973	0.0108,2.912	0.0018,1.240	0.0028,0	0.0043,1.223
		$3p+$	0.0116,−3.038	0.0114,−3.052	0.0114,−3.060	0.0113,−3.060	0.0119,−3.350	0.0121,−3.048
		triplet	0.0118,−3.038	0.0122,−3.017	0.0123,−3.087	0.0007,1.180	0.0010,0	0.0020,2.466
200	2	$3s$	0.0700,−2.110	0.0700,−2.109	0.0700,−2.109	0.0700,−2.114	0.0722,−2.134	0.0704,−2.105
		singlet	0.0705,−2.097	0.0711,−2.083	0.0716,−2.068	0.0520,−2.463	0.0669,π	0.0973,−2.552
		$3p-$	0.0080,0.158	0.0081,0.160	0.0081,0.158	0.0072,0.162	0.0076,−0.203	0.0086,0.135
		singlet	0.0081,0.213	0.0079,0.267	0.0084,0.262	0.0022,1.308	0.0035,0	0.0073,0.833
		$3p+$	0.0051,1.611	0.0051,1.613	0.0050,1.608	0.0048,1.604	0.0050,1.337	0.0054,1.594
		singlet	0.0052,1.631	0.0055,1.649	0.0055,1.681	0.0002,0.509	0.0001,0	0.0039,−0.026
		$3s$	0.0702,−2.106	0.0702,−2.104	0.0703,−2.104	0.0702,−2.110	0.0724,−2.131	0.0707,−2.101
		triplet	0.0707,−2.093	0.0713,−2.079	0.0718,−2.064	0.0522,−2.460	0.0672,π	0.0979,−2.550
		$3p-$	0.0079,0.166	0.0079,0.167	0.0079,0.166	0.0071,0.169	0.0075,−0.203	0.0084,0.141
		triplet	0.0079,0.220	0.0076,0.274	0.0082,0.284	0.0021,1.301	0.0033,0	0.0070,0.813
		$3p+$	0.0050,1.617	0.0051,1.619	0.0050,1.615	0.0048,1.610	0.0049,1.337	0.0053,1.598
		triplet	0.0052,1.637	0.0055,1.655	0.0055,1.685	0.002,0.596	0.0001,0	0.0039,−0.011
54.42	0	$3s$	0.1449,−1.337	0.1449,−1.340	0.1451,−1.341	0.1503,−1.457	0.1664,−1.442	0.1554,−1.310
		singlet	0.1453,−1.334	0.1481,−1.317	0.1424,−1.323	0.0644,−2.715	0.0706,π	0.0814,−2.736
		$3p$	0.0383,1.354	0.0385,1.348	0.0381,1.334	0.0347,1.284	0.0389,0.798	0.0475,1.241
		singlet	0.0375,1.347	0.0300,1.630	0.0416,1.339	0.0099,0.280	0.0110,0	0.0358,0.094
		$3s$	0.1450,−1.323	0.1458,−1.325	0.1460,−1.329	0.1512,−1.425	0.1681,−1.413	0.1567,−1.281
		triplet	0.1460,−1.315	0.1442,−1.315	0.1433,−1.310	0.0528,−2.791	0.0561,π	0.0748,−2.864
		$3p$	0.0371,1.376	0.0356,1.424	0.0356,1.403	0.0310,1.357	0.0350,0.798	0.0440,1.294
		triplet	0.0344,1.422	0.0379,1.402	0.0392,1.420	0.0100,0.216	0.0107,0	0.0271,0.091
54.42	1	$3s$	0.0472,−0.645	0.0473,−0.647	0.0455,−0.624	0.0598,−0.631	0.0709,−0.252	0.0387,−0.369
		singlet	0.0469,−0.657	0.0473,−0.664	0.0471,−0.656	0.0222,−0.170	0.0222,0	0.0500,−0.079
		$3p-$	0.0275,−1.704	0.0277,−1.703	0.0284,−1.663	0.0281,−1.829	0.0336,−2.329	0.0358,−1.769
		singlet	0.0262,−1.711	0.0264,−1.719	0.0264,−1.703	0.0099,0.314	0.0112,0	0.0041,1.367
		$3p+$	0.0397,−2.703	0.0397,−2.708	0.0373,−2.829	0.0358,−2.829	0.0409,3.056	0.0453,−2.813
		singlet	0.0414,−2.783	0.0418,−2.783	0.0413,−2.778	0.0031,0.131	0.0030,0	0.0329,3.137
		$3s$	0.0471,−0.552	0.0471,−0.554	0.0427,−0.589	0.0568,−0.575	0.0690,−0.191	0.0369,−0.281
		triplet	0.0443,−0.599	0.0446,−0.611	0.0444,−0.605	0.0191,−0.210	0.0185,0	0.0499,−0.088
		$3p-$	0.0247,−1.516	0.0250,−1.526	0.0262,−1.650	0.0251,−1.771	0.0299,−2.329	0.0321,−1.710
		triplet	0.0251,−1.660	0.0253,−1.661	0.0252,−1.644	0.0162,0.361	0.0188,0	0.0078,1.470
		$3p+$	0.0336,−2.395	0.0337,−2.413	0.0361,−2.731	0.0331,−2.763	0.0377,3.056	0.0424,−2.754
		triplet	0.0377,−2.712	0.0385,−2.717	0.0321,−2.713	0.0033,0.091	0.0030,0	0.0303,−3.133
	2	$3s$	0.1062,−2.297	0.1062,−2.296	0.1066,−2.287	0.1027,−2.356	0.1113,−2.412	0.1128,−2.288
		singlet	0.1066,−2.293	0.1068,−2.287	0.1069,−2.284	0.0779,2.599	0.0910,π	0.1249,−2.686
		$3p-$	0.0361,0.557	0.0363,0.557	0.0372,0.565	0.0310,0.479	0.0358,−0.068	0.0444,0.450
		singlet	0.0363,0.578	0.0368,0.599	0.0373,0.611	0.0181,0.549	0.0215,0	0.0441,0.304
		$3p+$	0.088,1.065	0.0088,1.061	0.0088,1.064	0.0086,1.116	0.0090,0.922	0.0085,1.150
		singlet	0.0089,1.077	0.0091,1.087	0.0090,1.077	0.0030,−1.1579	0.0030,π	0.0075,−0.769
		$3s$	0.1092,−2.285	0.1093,−2.284	0.1097,−2.275	0.1061,−2.341	0.1145,−2.397	0.1158,−2.278
		triplet	0.1098,−2.280	0.1099,−2.275	0.1101,−2.271	0.0809,−2.583	0.0954,π	0.1302,−2.666
		$3p-$	0.0338,0.598	0.0340,0.598	0.0349,0.607	0.0285,0.520	0.0331,−0.068	0.0409,0.479
		triplet	0.0339,0.617	0.0344,0.636	0.0348,0.649	0.0167,0.559	0.0199,0	0.0413,0.308
		$3p+$	0.0091,1.127	0.0090,1.124	0.0092,1.128	0.0086,1.157	0.0089,0.922	0.0089,1.177
		triplet	0.0091,1.139	0.0093,1.147	0.0092,1.138	0.0020,−1.404	0.0018,π	0.0069,−0.571

VI. APPROXIMATIONS TO THE COUPLED-CHANNELS SOLUTION

Various approximations to elastic and inelastic scattering have been used. Their main advantage is speed of computation, although this is only a minor advantage in comparison with the present coupled-channels method with modern computers.

When used in a realistic scattering problem the distorted-wave approximations should strictly include the effects of all channels in the distorting potentials. However, the additional polarization potentials make a minor difference and the static potential of the target is often used. The best distorted-wave approximation is to use the potential for the target in the appropriate state.[12] The second-order approximations require a sum and integral over all target states, which is sometimes calculated in the closure approximation[13] and sometimes included explicitly.[14]

We may consider the two-state coupled-channels problem for sodium at 54.42 eV as a model problem to which we test the value of various approximations. We cannot close the set of coupled integral equations with a state-dependent distorting potential. We choose U to be the average static potential for the ground state. The first-order solution of the coupled integral equations in the distorted-wave representation is called the DWBA. This approximation has been called first-order many-body theory.[15] It must be emphasized that the coupled-channels (CC) solution to the model problem is exact within the limitations of the numerical methods. The distorting potential is merely an aid to the convergence of the numerical method.

It is possible to make two better approximations than the DWBA. The first is the unitarized distorted-wave Born approximation (UDWB) in which the channels are coupled but only by on-shell amplitudes. The real part of the Green's function in the integral equations is neglected. This approximation involves little more computation than the DWBA and it is hard to imagine why it is not used more often. By contrast, the distorted-wave second Born approximation (DWSB) involves nearly as much computational labor as the full coupled-channels calculation, since the same off-shell amplitudes must be computed at all the quadrature points. Much of this labor could be saved by making a closure approximation, but this is quite inaccurate[14] and would be worthwhile only if DWSB is vastly superior to other approximations.

Figure 1 compares the DWBA, DWSB, and UDWB with the CC method. The corresponding plane-wave approximations are, respectively, the first-order Born approximation, the second-order Born approximation, and the unitarized Born approximation. They are compared with CC in Fig. 2. The first-order Born approximation (FBA) is of course much simpler than the others but cannot be taken seriously except for the dipole channel at small angles (momentum transfer $K < 0.35$ a.u.). Neither the unitarized Born approximation (UBA) nor the second-order Born approximation (SBA) are good approximations although the SBA bears some shape resemblance to the CC method.

The situation changes dramatically with the introduction of the distorting potential U. The DWBA is not very good for the elastic channel but could almost be considered a good approximation for the dipole excitation. The DWSB is a fair approximation in both channels and

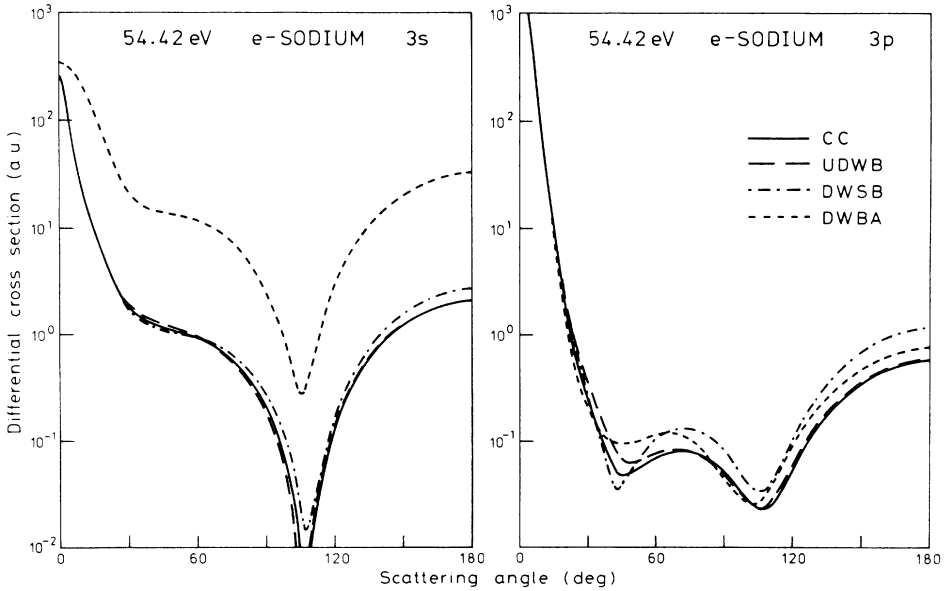

FIG. 1. Comparison of the differential cross sections in atomic units (a.u.) for the exact numerical solution (CC) for 54.42-eV electron scattering on the model channel space sodium $3s,3p$ with the unitarized distorted-wave Born (UDWB), distorted-wave second-order Born (DWSB), and distorted-wave Born (DWBA) approximations.

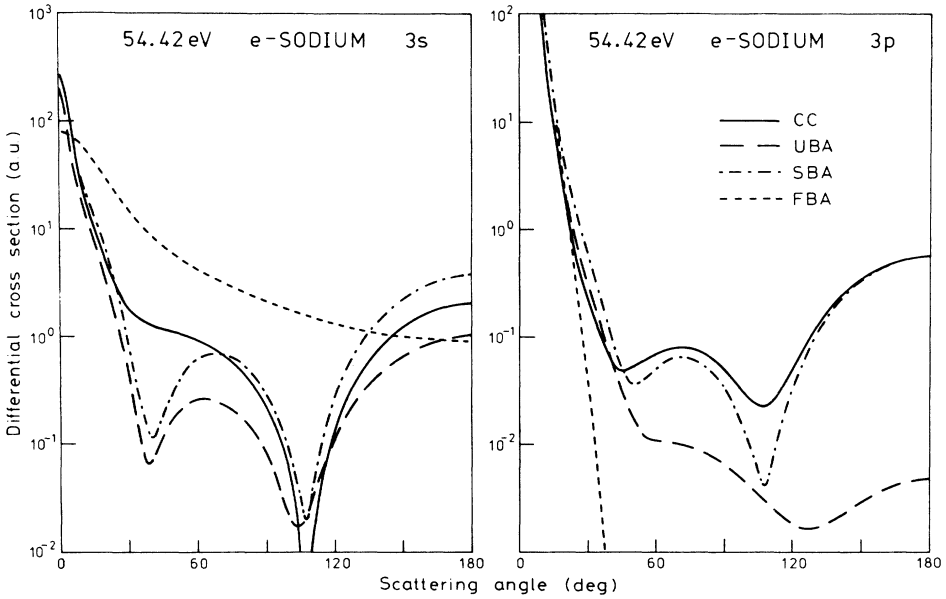

FIG. 2. Same as Fig. 1 for the plane-wave unitarized Born (UBA), second-order Born (SBA), and first-order Born (FBA) approximations.

the UDWB is a very good approximation. It is significant that the much-easier UDWB is considerably better than the DWSB.

The UDWB should be considered seriously for realistic problems. This conclusion is reinforced by a further calculation at 54.4 eV involving $3s$, $3p$, $4s$, and $3d$ channels, where it is again superior to the DWSB. For problems for which the continuum is important it has yet to be tested in the optical-potential formulation. The UDWB improves considerably on the DWBA for the elastic channel because it includes the effect of absorption of flux into inelastic channels.

VII. ELECTRON SCATTERING FROM CHARGED TARGETS

In this section we show preliminary results demonstrating that the momentum-space method for solving the CC equations can be applied to electron-ion collisions. We have applied the method to a three-state ($1s2s2p$) calculation of electron scattering from He^+ at incident energies of 54.42, 108.85, and 217.69 eV. The results will be compared with previous CC calculations in coordinate space by Burke, McVicar, and Smith[16] (hereafter referred to as BMS).

One feature of the method that is peculiar to ion targets is the presence of an infinite number of bound states in the spectral decomposition of the Green's function. The inclusion of these bound states is quite important for a correct description of electron-ion scattering. They give rise to an infinite series of Feshbach resonances associated with the temporary binding of the incident electron to an excited level of the target at incident energies smaller than the excitation energies of the target level. The present calculations are performed at incident energies above the $2s$ and $2p$ excitation threshold, and although this is outside the resonance region, the inclusion of a number of bound states was necessary to obtain converged results. The largest number of bound states were required at 54.42 eV, where nine s-wave, eight p-wave, seven d-wave, six f-wave, and five g-wave bound states were needed to obtain converged results. The number of bound states needed for converged results decreased with increasing incident energies. At 108.85 eV, five s-wave, four p-wave, three d-wave, two f-wave, and one g-wave bound states were sufficient, whereas at 217.69 eV only three s-wave, two p-wave, and one d-wave states were needed.

In Table III we study the convergence of the T-matrix elements with the number of quadrature points at $E_0=108.85$ eV. The same format as in Table II is used except there are no plane-wave or distorted-wave calculations. Only the Coulomb-wave representation is used. The unitarized Coulomb-Born approximation (UCBA), the first-order Coulomb-Born (CB), and the second-order Coulomb-Born (SCB) approximations are shown.

The agreement between the calculations using 16 and 24 off-shell continuum points is quite good for all values presented in Table III. The agreement between perturbation theory (UCBA, CB, and SCB) and the full solution is not good for the lowest partial waves, $J=0$ and 1. However, at $J=2$, the UCBA (and to a lesser extent the SCB) T matrix is starting to become a reasonable approximation to the full solution.

The partial cross sections for the $1s$-$2s$ and $1s$-$2p$ transitions are presented in Tables IV and V, respectively. Calculations using 16 and 24 off-shell continuum points are tabulated and compared to prior coordinate-space calculations of BMS. The present calculation agrees well with the BMS values at $E_0=108.85$ eV and $E_0=217.69$ eV for all J. At 54.42 eV, the present values are in quite

TABLE III. T-matrix elements (magnitude and phase) for electron scattering in the 1s, 2s, and 2p model of He^+. $E_0 = 108.85$ eV.

J	Channel	24 points	16 points	UCBA	CB	SCB
0	1s singlet	0.031 92,−2.400	0.031 95,−2.399	0.035 04,−2.425	0.037 79,−2.767	0.026 75,−2.210
	2s singlet	0.012 55,1.791	0.012 59,1.779	0.007 53,1.543	0.011 11,0.413	0.022 17,1.148
	2p singlet	0.013 58,0.814	0.013 55,0.803	0.007 89,0.618	0.009 14,−0.075	0.017 95,0.357
	1s singlet	0.055 25,−2.246	0.055 22,−2.246	0.043 92,−2.356	0.048 33,−2.767	0.060 97,−2.404
	2s triplet	0.004 20,2.120	0.004 24,2.104	0.006 82,1.590	0.010 31,0.413	0.014 44,2.069
	2p triplet	0.005 80,1.095	0.005 84,1.087	0.003 15,0.894	0.004 13,−0.075	0.008 89,0.499
1	1s singlet	0.003 28,−3.034	0.003 24,−3.031	0.002 25,−2.950	0.002 59,−3.346	0.003 62,−3.031
	2s singlet	0.010 98,0.199	0.011 00,0.201	0.009 76,0.122	0.010 91,−0.347	0.012 00,1.024
	2p − singlet	0.006 37,0.693	0.006 37,0.705	0.006 89,0.712	0.008 92,0.073	0.010 09,0.838
	2p + singlet	0.003 47,−0.324	0.003 38,−0.340	0.001 77,−0.952	0.000 93,−0.567	0.003 28,−0.956
	1s singlet	0.021 93,3.046	0.021 91,3.046	0.020 35,3.029	0.020 84,2.837	0.022 25,3.024
	2s triplet	0.005 52,0.460	0.005 50,0.458	0.004 24,0.320	0.004 87,−0.347	0.006 20,0.243
	2p − triplet	0.000 70,0.251	0.000 74,0.389	0.002 79,0.905	0.003 68,0.073	0.003 99,2.076
	2p + triplet	0.002 99,−0.028	0.002 97,−0.039	0.001 89,−0.270	0.001 82,−0.567	0.002 94,−0.418
2	1s singlet	0.001 40,−2.286	0.001 41,−2.274	0.001 38,−1.993	0.000 25,2.487	0.001 69,−2.514
	2s singlet	0.002 95,−0.400	0.003 01,−0.388	0.003 82,−0.402	0.004 22,−0.742	0.002 96,−0.184
	2p − singlet	0.013 61,−0.068	0.013 63,−0.068	0.013 15,−0.124	0.014 55,−0.522	0.015 62,−0.111
	2p + singlet	0.001 69,−2.942	0.001 70,−2.954	0.001 31,−2.695	0.000 89,−0.890	0.002 13,−3.226
	1s triplet	0.006 88,2.589	0.006 86,2.590	0.006 24,2.576	0.006 35,2.487	0.006 95,2.575
	2s triplet	0.004 42,−0.306	0.004 42,−0.302	0.003 88,−0.336	0.004 20,−0.742	0.004 78,−0.355
	2p − triplet	0.004 42,0.051	0.004 46,0.054	0.003 79,0.002	0.004 29,−0.522	0.005 36,−0.052
	2p + triplet	0.001 11,−1.042	0.001 09,−1.058	0.000 69,−1.426	0.000 34,−0.890	0.000 93,−1.440

good agreement for $J > 2$. For the low partial waves, there seem to be some problems in getting the present method to agree with BMS within a few percent. We believe that this is due to not having enough points in the momentum grid for solving the integral equations.

In conclusion, it has been demonstrated that the Coulomb-wave representation can be used to solve the CC equations for electron-ion collisions. It is expected that the method will be most useful at high impact energies where currently used methods (R matrix and linear algebraic)[17,18] become increasingly time consuming.

TABLE IV. Inelastic partial-wave cross sections 1s-2s for the scattering of He^+ in units of πa_0^2. s and t denote singlet and triplet, respectively.

J		16 points	24 points	BMS	16 points	24 points	BMS	16 points	24 points	BMS
			$E_0 = 54.42$ eV			$E_0 = 108.85$ eV			$E_0 = 217.69$ eV	
0	s	0.005 51	0.005 34	0.005 65	0.001 24	0.001 23	0.001 19	0.000 33	0.000 33	0.000 32
	t	0.000 46	0.000 46	0.000 28	0.000 42	0.000 41	0.000 36	0.000 26	0.000 25	0.000 23
1	s	0.004 74	0.004 76	0.004 57	0.002 84	0.002 82	0.002 74	0.000 91	0.000 90	0.000 89
	t	0.005 09	0.004 88	0.004 89	0.002 12	0.002 14	0.002 08	0.000 96	0.000 94	0.000 92
2	s	0.002 54	0.002 62	0.002 79	0.000 35	0.000 34	0.000 31	0.000 53	0.000 53	0.000 51
	t	0.002 97	0.002 86	0.002 78	0.002 29	0.002 29	0.002 21	0.001 16	0.001 14	0.001 11
3	s	0.001 05	0.001 05	0.001 11	0.000 06	0.000 06	0.000 05	0.000 21	0.000 21	0.000 20
	t	0.000 03	0.000 04	0.000 05	0.000 72	0.000 70	0.000 64	0.000 78	0.000 77	0.000 74
4	s	0.000 14	0.000 14	0.000 15	0.000 10	0.000 10	0.000 10	0.000 07	0.000 07	0.000 06
	t	0.000 20	0.000 20	0.000 22	0.000 18	0.000 17	0.000 15	0.000 39	0.000 38	0.000 35
5	s	0.000 02	0.000 02	0.000 02	0.000 08	0.000 08	0.000 08	0.000 03	0.000 03	0.000 03
	t	0.000 06	0.000 06	0.000 06	0.000 11	0.000 11	0.000 10	0.000 17	0.000 16	0.000 15

TABLE V. Inelastic partial-wave cross sections $1s$-$2p$ for the scattering of He^+ in units of πa_0^2. s and t denote singlet and triplet, respectively.

J		16 points	24 points	BMS	16 points	24 points	BMS	16 points	24 points	BMS
		$E_0=54.42$ eV			$E_0=108.85$ eV			$E_0=217.69$ eV		
0	s	0.004 90	0.004 98	0.005 15	0.001 43	0.001 44	0.001 46	0.000 23	0.000 24	0.000 24
	t	0.000 51	0.000 52	0.000 48	0.000 80	0.000 79	0.000 78	0.000 33	0.000 34	0.000 33
1	s	0.008 06	0.008 25	0.009 76	0.001 22	0.001 23	0.001 29	0.000 15	0.000 16	0.000 17
	t	0.002 42	0.002 20	0.002 58	0.000 66	0.000 66	0.000 68	0.000 22	0.000 23	0.000 23
2	s	0.037 00	0.037 91	0.038 15	0.007 37	0.007 33	0.007 29	0.001 00	0.001 02	0.001 02
	t	0.002 42	0.002 77	0.002 83	0.002 46	0.002 43	0.002 44	0.000 87	0.000 89	0.000 90
3	s	0.010 44	0.010 66	0.010 63	0.008 05	0.008 02	0.007 97	0.001 84	0.001 85	0.001 85
	t	0.013 00	0.013 70	0.013 46	0.007 87	0.007 81	0.007 78	0.002 41	0.002 43	0.002 43
4	s	0.002 46	0.002 50	0.002 49	0.005 70	0.005 70	0.005 67	0.002 20	0.002 21	0.002 21
	t	0.006 66	0.006 89	0.006 83	0.009 90	0.009 90	0.009 85	0.003 90	0.003 90	0.003 90
5	s	0.000 62	0.000 63	0.000 63	0.003 61	0.003 61	0.003 59	0.002 18	0.002 18	0.002 18
	t	0.001 91	0.001 95	0.001 94	0.008 44	0.008 44	0.008 40	0.004 67	0.004 67	0.004 68

VIII. CONCLUSIONS

This paper constitutes a sequel to I, which gave the details of the plane-wave representation of the coupled Lippmann-Schwinger equations for a finite discrete set of channels with a one-electron target. Here the method has been extended to the distorted-wave representation for a many-electron target described by configuration interaction. A detailed partial-wave treatment of the optical potential for excitation of the complementary set of channels in the distorted-wave Born approximation[19] will follow.

The distorted-wave representation is very useful in providing rapid convergence of the numerical solution of the coupled equations. Treating the truncated channel space as a model problem enables us to assess the validity of some common approximation methods for electron-atom scattering. For the case of $3s$ and $3p$ channels of sodium none of the first-order Born, second-order Born or unitarized Born approximations are adequate. However, the corresponding distorted-wave approximations are a vast improvement. The distorted-wave Born approximation is reasonable for the dipole excitation but not for elastic scattering. The distorted-wave second-order Born approximation is quite good for both and the much easier unitarized distorted-wave Born approximation is excellent.

For a charged target the representation must at least involve asymptotic Coulomb waves. Distorted waves with Coulomb boundary conditions are numerically difficult in long-range dipole integrals but the representation in terms of pure Coulomb waves is tractable. The Coulomb second-order Born and unitarized Coulomb Born approximations are quite close in usefulness to the corresponding distorted-wave approximations, indicating that the Coulomb potential already provides enough distortion to accelerate the on-shell convergence of the Lippmann-Schwinger equations.

ACKNOWLEDGMENTS

This project was supported by the Australian Research Council.

[1] I. E. McCarthy and A. T. Stelbovics, Phys. Rev. A **28**, 2693 (1983).
[2] J. Mitroy, I. E. McCarthy, and A. T. Stelbovics, J. Phys. B **19**, 335 (1986).
[3] B. H. Bransden and M. R. C. McDowell, Phys. Rep. **30C**, 207 (1977).
[4] R. R. Whitehead, A. Watt, B. J. Cole, and I. Morrison, Adv. Nucl. Phys. **9**, 123 (1979).
[5] P. G. Burke and W. D. Robb, Adv. At. Mol. Phys. **11**, 143 (1975).
[6] M. Gell-Mann and M. L. Goldberger, Phys. Rev. **91**, 398 (1953).
[7] L. J. Allen, I. Bray, and I. E. McCarthy, Phys. Rev. A **37**, 49 (1988).
[8] I. S. Gradshteyn and I. M. Ryzhik, *Tables of Integrals, Series and Products* (Academic, New York, 1965).
[9] K. Alder, A. Bohr, T. Huus, B. Mottelson, and A. Winther, Rev. Mod. Phys. **28**, 432 (1956).
[10] A. Burgess, D. G. Hummer, and J. A. Tully, Philos. Trans. R. Soc. A **266**, 225 (1970).
[11] M. Samuel and U. Smilansky, Comput. Phys. Commun. **2**, 455 (1971).
[12] D. H. Madison and W. N. Shelton, Phys. Rev. A **7**, 499 (1973).
[13] D. H. Madison and K. H. Winters, J. Phys. B **16**, 4437 (1983).
[14] D. H. Madison, J. A. Hughes, and D. S. McGinness, J. Phys. B **18**, 2737 (1985).
[15] G. Csanak, H. S. Taylor, and R. Yaris, Phys. Rev. A **3**, 1322 (1971).
[16] P. G. Burke, D. D. McVicar, and K. Smith, Proc. Phys. Soc. **83**, 397 (1964).
[17] M. J. Seaton, J. Phys. B **7**, 1817 (1974).
[18] M. A. Crees, M. J. Seaton, and P. M. H. Wilson, Comput. Phys. Commun. **15**, 23 (1978).
[19] I. Bray, D. H. Madison, and I. E. McCarthy (unpublished).